Journal of Solid State Chemistry 184 (2011) 1263–1272

Contents lists available at ScienceDirect

Journal of Solid State Chemistry

journal homepage: www.elsevier.com/locate/jssc

Synthesis, crystal structures and characterization of four coordination polymers based on 5-amino-2,4,6-triiodoisophthalic acid

Kou-Lin Zhang [a,*], Yan Chang [a], Jing-Bo Zhang [a], Li-Min Yuan [b], Ye Deng [a], Guo-Wang Diao [a,*], Seik Weng Ng [c]

[a] Key Laboratory of Environmental Material and Environmental Engineering of Jiangsu Province, College of Chemistry and Chemical Engineering, Yangzhou University, Yangzhou 225002, China
[b] Test and Analysis Center, Yangzhou University, Yangzhou 225002, China
[c] Department of Chemistry, University of Malaya, 50603 Kuala Lumpur, Malaysia

ARTICLE INFO

Article history:
Received 22 December 2010
Received in revised form
19 March 2011
Accepted 27 March 2011
Available online 6 April 2011

Keywords:
Synthesis
Crystal structures
Characterization
Coordination polymers
Decameric water clusters
Fluorescence spectra

ABSTRACT

One homochiral 1D coordination polymer [Cu(ATIBDC)(2,2′-bipy)]·3H_2O·CH_3OH (**1**) and three achiral 1D coordination polymers: [Cd(ATIBDC)(2,2′-bipy)(H_2O)]·3H_2O (**2**), [Cd(ATIBDC)(phen)(H_2O)]·4H_2O (**3**), and [Mn(ATIBDC)(phen)$_2$]·5H_2O (**4**) have been synthesized and characterized (H_2ATIBDC= 5-amino-2,4,6-triiodoisophthalic acid, 2,2′-bipy=2,2′-bipyridine, and phen=1,10-phenanthroline). Extended high dimensional network architectures are further constructed with the help of weak secondary interactions, such as hydrogen bonding, aromatic stacking, and halogen bonding (C–I…π and C–I…N/O). Complex **1** crystallizes in the monoclinic system with chiral space group *P*2(1) and exhibits a right-handed 2_1 helical chain structure. The homochirality of **1** was confirmed by CD spectrum. Interestingly, two new configurations of decameric water cluster are found in **3** and **4**. The acyclic tetrameric cluster (H_2O)$_3$(CH_3OH) in **1** and (H_2O)$_4$ in **2** array into highly ordered helical infinite chains. Thermal stabilities of all the complexes have been studied. Solid state fluorescent properties of the Cd(II) complexes have been explored.

1. Introduction

Investigations on small hydrogen-bonded water clusters have been a subject of both theoretical and experimental research, as their structural information is the first step toward understanding the behavior of bulk water [1,2]. Meanwhile, the aim of contemporary supramolecular chemistry and crystal engineering is the development of new crystalline materials with various functions and possible applications such as molecular adsorption, magnetism, nonlinear optics, molecular sensing, heterogeneous catalysis, and photoactive materials although the rational design and synthesis of metal-organic frameworks (MOFs) with target structure and function still remains a long-term challenge [3–5]. The construction of supramolecular architectures depends on the combination of several factors, such as the coordination geometry of metal ions, the nature of organic ligands, the use of noncovalent interactions, and sometimes the ratio between metal salt and ligand [6,7]. So, understanding how these considerations affect metal coordination and influence crystal packing is at the forefront of controlling coordination supramolecular arrays. It has been documented that the geometries of organic ligands play crucial roles in determining the resulted polymeric structures. Thus, much effort has been devoted to modify the building blocks and to control the assembled motifs for required products *via* selecting different organic ligands. In this context, the rational design of organic ligands has great effect on the formation of desirable supramolecular networks. Therefore, the prospect of tuning the architectures and properties of MOFs through change of organic ligands provides an impetus for further research on metal-organic supramolecular complexes [8].

At present, we are focusing our attention on using iodine-containing 5-amino-2,4,6-triiodoisophthalic acid (H_2ATIBDC) as the organic moiety to react with transition metal ions in the presence of N-donor auxiliary ligands, which is based mostly on the following considerations. (1) The three I atoms in H_2ATIBDC are potential interaction sites for forming C–I…N/O, C–I…I or C–I…π halogen bonds which may help to extend the linkage into high dimensional supramolecular network due to their specific directional nature and relatively high halogen bonding energy [9]. It should be noted that the Cl/Br-assisted supramolecular architectures with transition metal ions are reported extensively, while the I-assisted supramolecular complexes are relatively rare. So, it is worthwhile to carry out further systematic study about the roles of three I atoms in the supramolecular assembly. (2) The anion ATIBDC^{2-} is a rigid aromatic dicarboxylate ligand and can play the role of a bridging rod. Therefore, a structural prediction

* Corresponding authors. Fax: +86 0514 87975244.
E-mail addresses: klzhang@yzu.edu.cn, koulinzhang2002@yahoo.com (K.-L. Zhang).

0022-4596/$ - see front matter © 2011 Elsevier Inc. All rights reserved.
doi:10.1016/j.jssc.2011.03.050

of the resulting polymeric complexes may be possible to some extent. Furthermore, due to the presence of aromatic/hetero rings of $ATIBDC^{2-}$ and N-donor auxiliary ligand in the assembled system, the delicate $\pi\ldots\pi$ stacking interactions are available to play a significant role in regulating the resulting supramolecular networks, which are also important in constructing and stabilizing the biological systems [10]. Several novel complexes with the $ATIBDC^{2-}$ ligand have been reported [11].

We have finished a systematic study about the lead(II) complexes with $H_2ATIBDC$ [12]. Herein we describe our recent systematic research work of the synthesis, crystallography, and properties of four supramolecular transition metal complexes with $H_2ATIBDC$ in order to further understand the coordination chemistry of $H_2ATIBDC$, the role of three I atoms in the supramolecular assembly, and synthesize novel complexes with good physical properties. With the introduction of auxiliary chelating ligands, 2,2′-bipyridine (2,2′-bipy) and 1,10-phenanthroline (phen), one homochiral 1D coordination polymer, $[Cu(ATIBDC)(2,2'\text{-bipy})]\cdot 3H_2O\cdot CH_3OH$ (**1**), and three achiral 1D coordination polymers: $[Cd(ATIBDC)(2,2'\text{-bipy})(H_2O)]\cdot 3H_2O$ (**2**), $[Cd(ATIBDC)(phen)(H_2O)]\cdot 4H_2O$ (**3**), and $[Mn(ATIBDC)(phen)_2]\cdot 5H_2O$ (**4**) have been obtained. We attempt to demonstrate the roles of supramolecular interactions (aromatic stacking, hydrogen bonding and halogen bonding) in engineering the resultant network architectures. Remarkably, two new conformations of decameric water cluster were found in **3** and **4**. The tetrameric cluster $(H_2O)_3(CH_3OH)$ in the chiral complex **1** and $(H_2O)_4$ in **2** assemble into highly ordered 2_1 helical chains. Solid state fluorescent properties of the Cd(II) complexes have been investigated.

2. Experimental section

2.1. Materials and measurements

The reagents were purchased commercially. Elemental analyses (C, H, and N) were carried out on a 240 C Elemental analyzer. FT-IR spectra (400–4000 cm^{-1}) were recorded from KBr pellet in Magna 750 FT-IR spectrophotometer. Solid state fluorescent spectra were recorded using an F 4500 fluorescence spectrometer. Thermogravimetric analysis was taken on NETZSCH STA 409 PG/PC instrument from room temperature to 800 °C at a heating rate of 10 °C/min in N_2. Solid state Circular Dichroism spectrum was recorded using an Jasco J-810 CD spectrometer.

2.2. Crystal structure determination

Crystallographic data were collected with a Siemens SMART CCD diffractometer using graphite-monochromated (Mo-$K\alpha$) radiation (λ=0.71073 Å), ψ and ω scans mode. The structures were solved by direct methods and refined by Full-Matrix least-squares on F^2 method using SHELXL-97 program [13]. Intensity data were corrected for Lorenz and polarization effects and a multi-scan absorption correction was performed. All non-hydrogen atoms were refined anisotropically. The carbon-bound hydrogen atoms of all the complexes and oxygen-bound hydrogen atom of methanol in **1** were added geometrically and allowed to ride on their respective parent atoms. The oxygen-bound hydrogen atoms of water molecules were located in the difference Fourier map and then kept fixed. The contribution of these hydrogen atoms was included in the structure factor calculations. Details of crystal data, collection and refinement are listed in Table 1.

2.3. Synthesis of the complexes

*$[Cu(ATIBDC)(2,2'\text{-bipy})]\cdot 3H_2O\cdot CH_3OH$ (**1**)*: An aqueous solution of $Cu(NO_3)_2\cdot 3H_2O$ (0.036 g, 0.150 mmol) in water (4 ml) was

Table 1
Crystallographic and structure refinement data for **1–4**.

	1	**2**
Empirical formula	$C_{19}H_{20}CuI_3N_3O_8$	$C_{18}H_{18}CdI_3N_3O_8$
Formula weight	862.62	897.45
Temperature (K)	293(2)	293(2)
Wavelength (Å)	0.71073	0.71073
Crystal system	Monoclinic	Orthorhombic
Space group	$P2_1$	$Pna2_1$
a (Å)	9.0560(6)	17.4570(17)
b (Å)	14.1567(10)	9.6129(10)
c (Å)	10.2238(7)	14.4613(14)
α (deg.)	90	90
β (deg.)	107.8080(10)	90
γ (deg.)	90	90
Volume (Å^3)	1247.92(15)	2426.8(4)
Z	2	4
D_{calc} (mg/m^3)	2.296	2.456
Absorption coeff. (mm^{-1})	4.635	4.765
F(0 0 0)	814	1672
θ Range for data collection (deg.)	2.09–28.33	2.33–27.50
Index ranges	$-8\le h\le 12$ $-18\le k\le 18$ $-13\le l\le 11$	$-22\le h\le 20$ $-12\le k\le 12$ $-18\le l\le 18$
Reflections collected	8227	20,432
Unique (R_{int})	5631 [R(int)=0.0871]	5497 [R(int)=0.0577]
Completeness to θ=27.5	98.30%	100.00%
Max. and min. transmission	0.523 and 0.375	0.467 and 0.401
Data $I>2\sigma(I)$/restraints/parameters	4235/10/309	4077/25/298
Goodness-of-fit on F^2	0.936	1.049
Flack para	−0.06(4)	−0.09(4)
Final R indices [$I>2\sigma(I)$]	R_1=0.0586 wR_2=0.1372	R_1=0.0440 wR_2=0.0797
R indices (all data)	R_1=0.0734 wR_2=0.1452	R_1=0.0698 wR_2=0.0899
Largest diff. peak and hole (e Å^{-3})	1.328 and −1.478	1.813 and −1.809
	3	**4**
Empirical formula	$C_{20}H_{20}Cd\ I_3N_3O_9$	$C_{32}H_{28}I_3MnN_5O_9$
Formula weight	939.5	1062.23
Temperature (K)	293(2)	293(2)
Wavelength (Å)	0.71073	0.71073
Crystal system	Monoclinic	Monoclinic
Space group	$P2_1/c$	$P2_1/c$
a (Å)	8.9247(6)	9.7187(7)
b (Å)	14.8943(10)	18.5089(14)
c (Å)	20.3308(14)	20.2204(16)
α (deg.)	90	90
β (deg.)	98.8090(10)	101.865
γ (deg.)	90	90
Volume (Å^3)	2670.6(3)	3559.6(5)
Z	4	4
D_{calc} (Mg/m^3)	2.337	1.982
Absorption coeff. (mm^{-1})	4.338	3.032
F(0 0 0)	1760	2044
θ Range for data collection (deg.)	1.70–27.50	1.51–27.50
Index ranges	$-11\le h\le 11$ $-17\le k\le 19$ $-26\le l\le 26$	$-12\le h\le 11$ $-24\le k\le 23$ $-26\le l\le 26$
Reflections collected	22,909	30,915
Unique (R_{int})	6115 [R(int)=0.0351]	8140 [R(int)=0.0476]
Completeness to θ=27.5	99.50%	99.50%
Max. and min. transmission	0.771 and 0.570	0.809 and 0.681
Data $I>2\sigma(I)$/restraints/parameters	4773/30/325	5501/16/475
Goodness-of-fit on F^2	1.031	1.014
Final R indices [$I>2\sigma(I)$]	R_1=0.0290 wR_2=0.0621	R_1=0.0345 wR_2=0.0640
R indices (all data)	R_1=0.0438 wR_2=0.0677	R_1=0.0661 wR_2=0.0743
Largest diff. peak and hole (e Å^{-3})	0.910 and −0.875	0.775 and −0.847

added to a mixture of H_2ATIBDC (0.056 g, 0.100 mmol) in water (5 ml) and NaOH (0.4 ml, 0.5 mol/l) whilst stirring. To this solution 2,2′-bipy (0.016 g, 0.100 mmol) in methanol (5 ml) was added and then filtered. Blue block crystals were collected (61% based on H_2ATIBDC). Anal. Calc. for $C_{19}H_{20}CuI_3N_3O_8$: C, 26.46; H, 2.34; N, 4.87; found: C, 26.40; H, 2.29; N, 4.78%.

[Cd(ATIBDC)(2,2′-bipy)(H_2O)]·3H_2O (***2***): Complex **2** can be obtained following the same synthetic procedure as that for **1** except that $CdCl_2 \cdot 2.5H_2O$ (0.011 g, 0.050 mmol), 2,2′-bipy (0.008 g, 0.050 mmol), H_2ATIBDC (0.056 g, 0.100 mmol), and NaOH (0.4 ml, 0.5 mol/l) were used. Pale yellow block crystals were formed (67% based on $CdCl_2 \cdot 2.5H_2O$). Anal. Calc. for $C_{18}H_{18}CdI_3N_3O_8$: C, 24.09; H, 2.02; N, 4.68; found: C, 23.93; H, 2.11; N, 4.58%.

[Cd(ATIBDC)(phen)(H_2O)]·4H_2O (***3***): Complex **3** can be obtained following almost the same synthetic procedure as that for **1** except that $CdCl_2 \cdot 2.5H_2O$ (0.046 g, 0.200 mmol), phen (0.010 g, 0.050 mmol), H_2ATIBDC (0.056 g, 0.100 mmol), and NaOH (0.4 ml, 0.5 mol/l) were used. Pale yellow crystals were formed (59% based on phen). Anal. Calc. for $C_{20}H_{20}CdI_3N_3O_9$: C, 25.57; H, 2.15; N, 4.47; found: C, 25.49; H, 2.10; N, 4.36%.

[Mn(ATIBDC)(phen)$_2$]·5H_2O (***4***): A mixture of H_2ATIBDC (0.056 g, 0.100 mmol) in water (4 ml) and NaOH (0.1 ml, 0.5 mol/l) was added to an aqueous solution of $MnCl_2 \cdot 4H_2O$ (0.020 g, 0.100 mmol) in water (3 ml) whilst stirring. To this solution phen (0.010 g, 0.050 mmol) in water (4 ml) was then added. The filtrate was kept at ambient temperature for several days and pale yellow crystals were formed (54% based on phen). Anal. Calc. for $C_{32}H_{28}I_3MnN_5O_9$: C, 36.18; H, 2.66; N, 6.59; found: C, 36.09; H, 2.59; N, 6.68%.

3. Results and discussion

3.1. Synthesis

The formation of the products is sensitive to synthetic conditions. The hydrothermal method is not suitable for the synthesis of **1**–**4** since the ligand ATIBDC^{2-} decomposes under hydrothermal condition. Therefore, complexes **1**–**4** have been obtained under ambient conditions. NaOH is used to neutralize the acid. Interestingly, the molar ratio of H_2ATIBDC:NaOH is important for the formation of **1**–**4** (1:2 for **1**–**3** and 2:1 for **4**). Otherwise the polycrystals or cotton-like solids are obtained.

It should be noted that complex **1** can only be obtained in the water–methanol system although several systems have been tried (such as water, water–ethanol, water–DMF, and water–CH_3CN). This indicates that methanol plays a critical role in the construction of **1**.

Several molar ratios of Cd(II):H_2ATIBDC:phen:NaOH (2:0.5:1:1, 2:0.5:1:2, 2:1:1:1, and 2:2:1:1) have been used during the synthesis of **3**, but only the ratio of 2:0.5:1:1 leads to the formation of single-crystal. This reveals that the molar ratio of the reactants has great influence on the construction of **3**.

3.2. Crystal structure descriptions

Structure of [Cu(ATIBDC)(2,2′-bipy)]·3H_2O·CH_3OH (***1***): At present, the design and synthesis of chiral self-assembling systems is one of the most challenging tasks of crystal engineering, among which homochiral MOFs have prompted great enthusiasm particularly for their industrial applications, such as enantioselective catalysis and separation [14]. Generally, chiral architectures are realized through achiral building blocks or through chiral building blocks. Fortunately, the reaction between Cu(II) and ATIBDC^{2-} ligand in the presence of auxiliary ligand 2,2′-bipy leads to the formation of homochiral MOF (**1**), which crystallizes in the monoclinic system with chiral space group *P*2(1) and features a right-handed 2_1 helical chain structure consisting of one crystallographically independent Cu(II) ion, one 2,2′-bipy ligand, one ATIBDC^{2-} ligand, three lattice water, and one CH_3OH.

The Cu(II) ion is six-coordinated by two nitrogen atoms from one 2,2′-bipy ligand and four oxygen atoms from two distinct ATIBDC^{2-} ligands and shows a greatly distorted octahedral geometry (CuO_4N_2), in which the axial positions are occupied by O1 and O4 atoms (Fig. 1A). Both Cu–N bond lengths [Cu1–N1 1.973(10), Cu1–N2 1.997(10) Å] and equatorial Cu–O bond lengths [Cu1–O2#1 1.954(8), Cu1–O3 2.014(8) Å] are all within the normal ranges [15]. It should be noted that the equatorial Cu–O bond lengths are comparable with an average distance of 1.984 Å, which is significantly shorter than those of the axial weak bonds [Cu1–O4 2.407(9), Cu1–O1#1 2.829(1) Å] (Table S1).

The ligand ATIBDC^{2-} coordinates to Cu(II) in tetradentate (k^2)–(k^2)–μ_2 bridging mode to form a right-handed helical chain (Fig. 1B, Scheme 1). All chains parallel with each other in the structure. Adjacent chains are linked by N3–H3B…O4 [3.054(14) Å] hydrogen bonds and $\pi \cdots \pi$ interactions between the benzene ring of ATIBDC^{2-} and the pyridyl ring of 2,2′-bipy with the centroid–centroid distance of 3.728(2) Å to give a 2D supramolecular wavy layer along *a* direction (Fig. 1C). Helical copper(II) chains connect each other through such supramolecular interactions, which make the neighboring helices possess the same chirality.

Fig. 1D displays the coordination environment of the helical water-methanol chain consisting of the tetrameric acyclic water-methanol cluster $(H_2O)_3CH_3OH$. This can be defined as C4 chain [2f]. The individual tetrameric subunit is composed of three lattice water molecules and one methanol molecule. Both the three lattice water molecules and methanol act as an acceptor as well as a donor in the hydrogen bonding scheme. Interestingly, the tetrameric water-methanol cluster $(H_2O)_3CH_3OH$ further assembles into an infinite hydrogen-bonded right-handed 2_1 helical chain along *b* direction, which links the adjacent supramolecular wavy layers into 3D supramolecular network through the hydrogen bonding between the lattice water molecules and carboxylate oxygen atoms [O5–H5B…O2 2.854(14), O6–H6B…O3 2.951(14), O7–H7B…O1 2.858(15) Å] (Fig. 1E, Table S2). From another point of view, both water and methanol molecules can be viewed as space fillers in this structure where there are cavities with an appropriate size for hosting them. The C4 helical chain fits very well in the network and at the same time interacts strongly with the environment. This may explain why this complex readily crystallizes in aqueous methanol and no crystals are formed when other alcohols are used. So, the existence of 1D water-methanol aggregate in this structure may have an important effect on consolidating the overall 3D supramolecular network.

It should be mentioned that the halogen bond exists between I2 and O7 [C13–I2…O7 3.196(3) Å]. Thus, O5 and O6 possess tricoordination, O7 shows tetracoordination, and O8 exhibits two-coordination.

The distance between the H2 attached to C2 and the centroid of pyridyl ring (C6–C10N2) is 2.976(2) Å, which reveals the existence of C2–H2…π interaction between the adjacent wavy layers. The C–H…π interaction further directs and stabilizes the 3D supramolecular network.

Thus, complex **1** possesses a chiral supramolecular architecture may be due to the supramolecular interactions between the helical Cu(II) and water–methanol chains, through which the same chirality is preserved.

Structure of [Cd(ATIBDC)(2,2′-bipy)(H_2O)]·3H_2O (***2***): Complex **2** exhibits a helical chain structure. In the asymmetrical unit, there are one Cd(II) atom, one ATIBDC^{2-} ligand, one 2,2′-bipy ligand, one coordinated water and three lattice water molecules (Fig. 2A, Table S1). Each Cd(II) atom is seven-coordinated by two

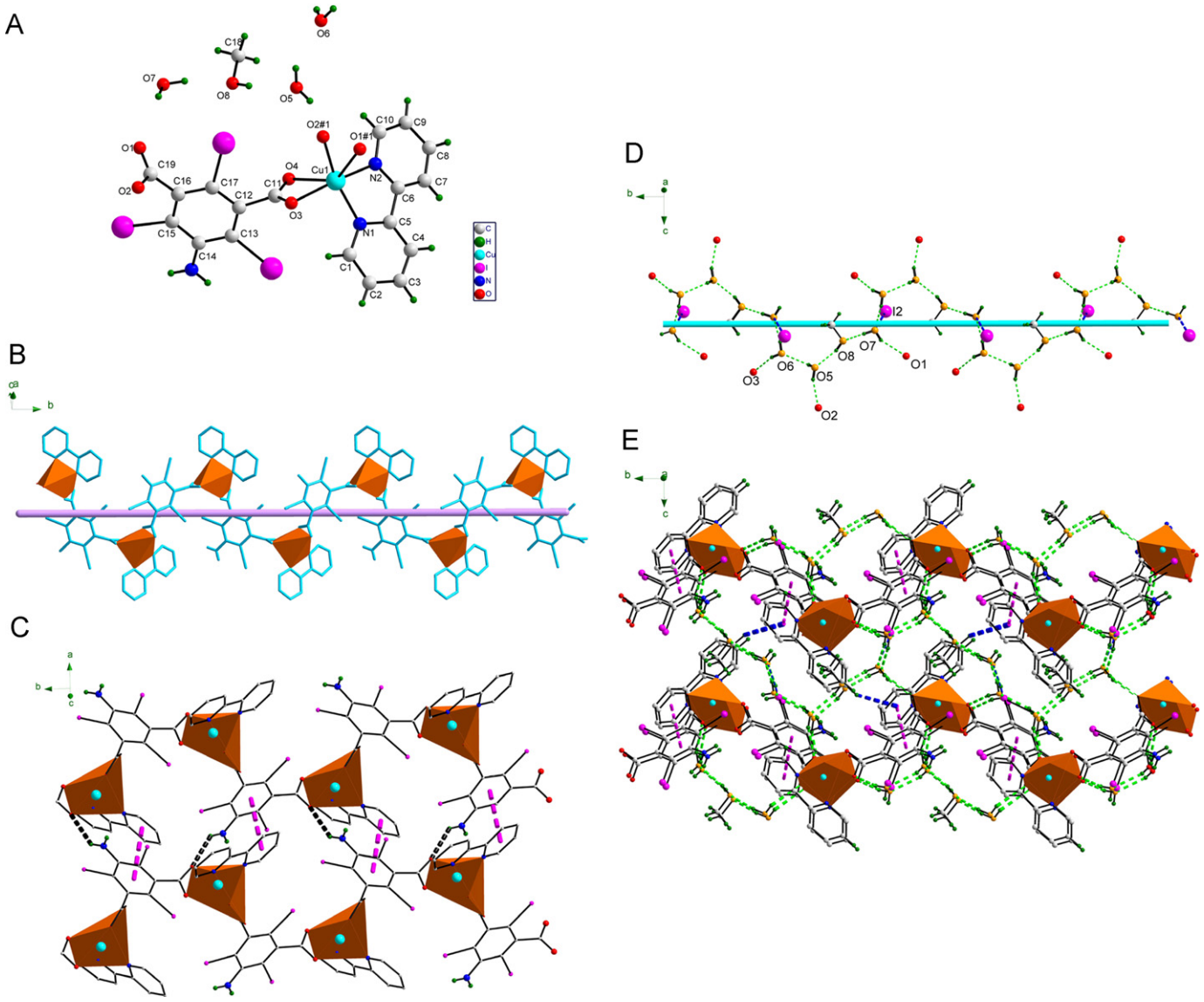

Fig. 1. (A) The coordination environment of Cu(II) in **1**. Symmetry operator: #1 $-x+1, y+1/2, -z+1$. (B) 1D right-handed helical chain. The solid line represents 2_1 helice. (C) 2D supramolecular layer formed through the $\pi\ldots\pi$ stacking interactions and N–H…O hydrogen bonds between 1D right-handed helical chains. (D) Perspective view of the hydrogen-bonded right-handed helical water-methanol chain. (E) 3D supramolecular network, showing the 1D hydrogen-bonded helical water–methanol chain and C–H…π interaction connecting the adjacent 2D supramolecular layers.

2,2′-bipyridyl nitrogen atoms, one oxygen atom from the coordinated water, and four oxygen atoms from two different ATIBDC^{2-} ligands to furnish a distorted [CdN2O5] geometry. The ATIBDC^{2-} ligand bridges the Cd(II) atoms in bischelating (k^2)–(k^2)–μ_2 mode to form a helical chain (Scheme 1). The nearest Cd…Cd distance within the chain is 9.888 Å.

The individual tetrameric $(H_2O)_4$ cluster consists of one coordinated water and three lattice water molecules. It is interesting that the tetrameric water cluster assembles into an infinit helical chain (Fig. 2B). This can be defined as a C4 water chain [2f]. The O…O distances range from 2.830 to 3.031 Å with an average O…O distance of 2.805 Å, which is comparable to those for the ice II phase (2.77–2.84 Å) [16]. In addition, both O2W and O4W are hydrogen-bonded to two coordinated carboxylate oxygen atoms of two neighboring chains by O2W–H2W2…O1 and O4W–H4W1…O2. As a result, the water chains serve as a glue to form the overall 2D supramolecular layer (Fig. 2C). The hydrogen-bonding interactions play an important role in stabilizing the solid-state structure.

The most important characteristics of this structure is that 1D chains within the layer are parallel with each other, but the chains of the adjacent layers are not. The chains in the adjacent layers recognize each other through the strong offset $\pi\ldots\pi$ stacking interactions (the centroid–centroid distance between the pyridyl ring C14–C18N3 and benzyl ring of ATIBDC^{2-} ligand is 3.590(3) Å), ultimately leading to a 3D supramolecular MOF with 1D channels along two directions (Fig. 2D–F). The lattice water molecules lie in the channel.

*Structure of [Cd(ATIBDC)(phen)(H_2O)]·4H_2O (**3**).* As shown in Fig. 3A, complex **3** contains one unique Cd(II) atom, one ATIBDC^{2-} ligand, one chelated phen ligand, one coordinated water, and four lattice water molecules in each asymmetric unit. The Cd(II) atom shows an octahedral coordination geometry [CdN_2O_4] completed by three carboxylate oxygen atoms from two ATIBDC^{2-} ligands, one O atom from water, and two N atoms from phen. The distances of Cd–$O_{carboxylate}$ and Cd–$N_{2,2'\text{-bipy}}$ are within the normal ranges (Table S1) [17]. The two carboxylate groups of the ATIBDC^{2-} ligand coordinate to the Cd atoms in monodentate (k^1)

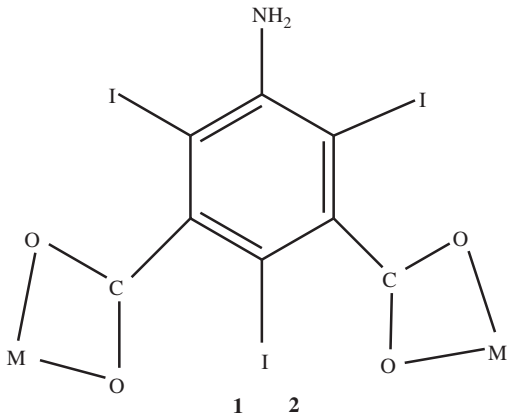

1 **2**

(k^2)-(k^2)-μ_2-ATIBDC^{2-}

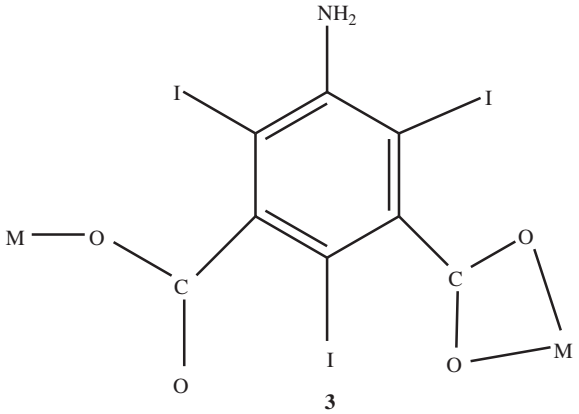

3

(k^2)-(k^1)-μ_2-ATIBDC^{2-}

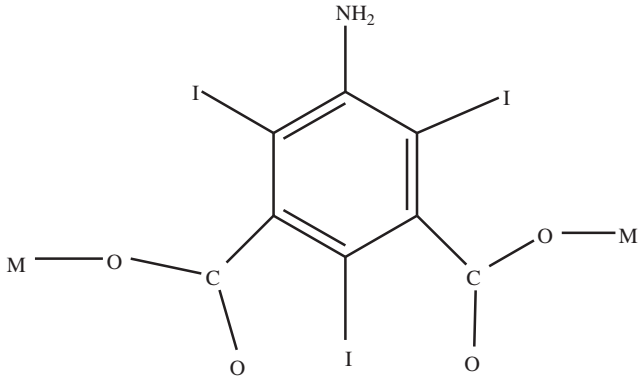

4

(k^1)-(k^1)-μ_2-ATIBDC^{2}

Scheme 1. Schematic representation of the coordination modes of the ATIBDC^{2-} ligand in **1**–**4**.

and bichelating (k^2) coordination mode, respectively. Thus, the helical chain was formed. The intrachain nearest Cd…Cd distance is 9.299(6) Å. The chains parallel with each other. Adjacent chains are linked by $\pi\ldots\pi$ interactions between the aromatic ring of ATIBDC^{2-} and pyridyl ring (C9–C13N2) of phen (the centroid–centroid distance: 3.542(2) Å) to give a 2D supramolecular wavy layer (Fig. 3B).

The phen ligands are alternately located at both sides of this 2D pattern in a slanted fashion (Fig. 3C). It should be mentioned that, due to the helical nature of the coordination chain, the phen segments in each chain are stretched outwards to produce the recognition sites for aromatic stacking with those from two neighboring chains in the adjacent layers. So, the chains in the adjacent layers parallel and recognize each other through the offset $\pi\ldots\pi$ stacking interactions between the aromatic rings of phen ligands (the distance between the centroids of C2–C7 and C9–C13N2: 3.653(2) Å), which is quite different from the structure of **1**. So in this manner, these 2D supramolecular coordination layers, being organized in a sequence of A(–A)A(–A) (centrosymmetry operation), are extended into a 3D supramolecular MOF with 1D channels. The lattice water molecules occupy in the channel.

The Cd(II)-coordinated water O1W, four lattice water molecules (O2W, O3W, O4W, O5W), and their symmetric equivalents together form a decameric water cluster. At the center of the cluster is a four-membered planar water ring (two O2W and two O4W) which shares two opposite edges (O2W…O4W) with two symmetrical parallel cyclic five-membered planar water rings (O1W–O5W).

The cyclic tetrameric water ring locates in the symmetrical center. Both theoretical calculations and vibration rotation tunneling spectroscopy of water tetramers in the gas phase indicate a quasiplanar structure, in which each water molecule forms two hydrogen bonds, one as a donor and the other as an acceptor. The average O–H…O bond length in the tetramer is estimated to be 2.79 Å [18]. It is of interest that the hydrogen-bonding motif of the water tetramer presented herein, in which each water molecule is involved in the formation of three hydrogen bonds with the adjacent water molecules, is actually two dimers connected to each other and almost the same as the theoretically predicted or experimentally observed structure in the gas phase.

The O…O distance in the decameric water cluster ranges from 2.573 to 2.917 Å, resulting in an average O…O distance of 2.779 Å which is very close to the corresponding value of 2.759 Å found in ice *Ih* [19] (Table S2).

In addition, the coordinated O1W forms an intramolecular hydrogen bond with the uncoordinated carboxylate O2 atom [O1W–H11…O2 2.717(4) Å], while the lattice water molecules O4W and O5W are H-bonded to the coordinated-carboxylate oxygen atoms O1 and O4, respectively [O5W–H51…O1 2.780(5) Å, O4W–H41…O4 2.811(5) Å]. All the five crystal water molecules act as an acceptor as well as a donor in the hydrogen bonding pattern. Furthermore, O2W is also halogen-bonded to I2 atom (I2…O2W 3.272 Å). So, both O1W and O5W possess tricoordination, O3W shows two coordination. If the C5–I2…O2W halogen bond is taken into consideration, both O2W and O4W show tetracoordination.

To the best of our knowledge, the reported conformations of water decamer are an adamantanoid "ice-like" cage, "opened-cube", endohedral clusterization "molecule ice", a cyclic decamer with boat-chair-boat conformation, a discrete 2D sheetlike fragement, nonplanar eight-membered ring and two water molecules, infinite chains, two parallel cyclic pentamers with staggered conformation, decameric water ring, and a decameric water cluster containing a quasiplanar six-membered ring [19]. The conformation of the decameric water cluster presented here is quite different from the reported one shaped as two parallel cyclic pentamers with staggered conformation [19h]. So, this decameric water cluster exhibits a new kind of structure which has not been speculated previously.

*Structure of [Mn(ATIBDC)(phen)$_2$]·5H$_2$O (**4**)*: Complex **4** crystallizes in the monoclinic system with space group *P*2(1)/*c* and exhibits helical chain structure. Each Mn(II) center is six-coordinated by four nitrogen atoms from a pair of phen chelating ligands and two oxygen atoms from two carboxylate groups of two different ATIBDC^{2-} ligands, adopting a distorted octahedral coordination geometry (Fig. 4A). The Mn–O distances are greatly shorter than those of Mn–N (Table S1). Each ATIBDC^{2-} ligand

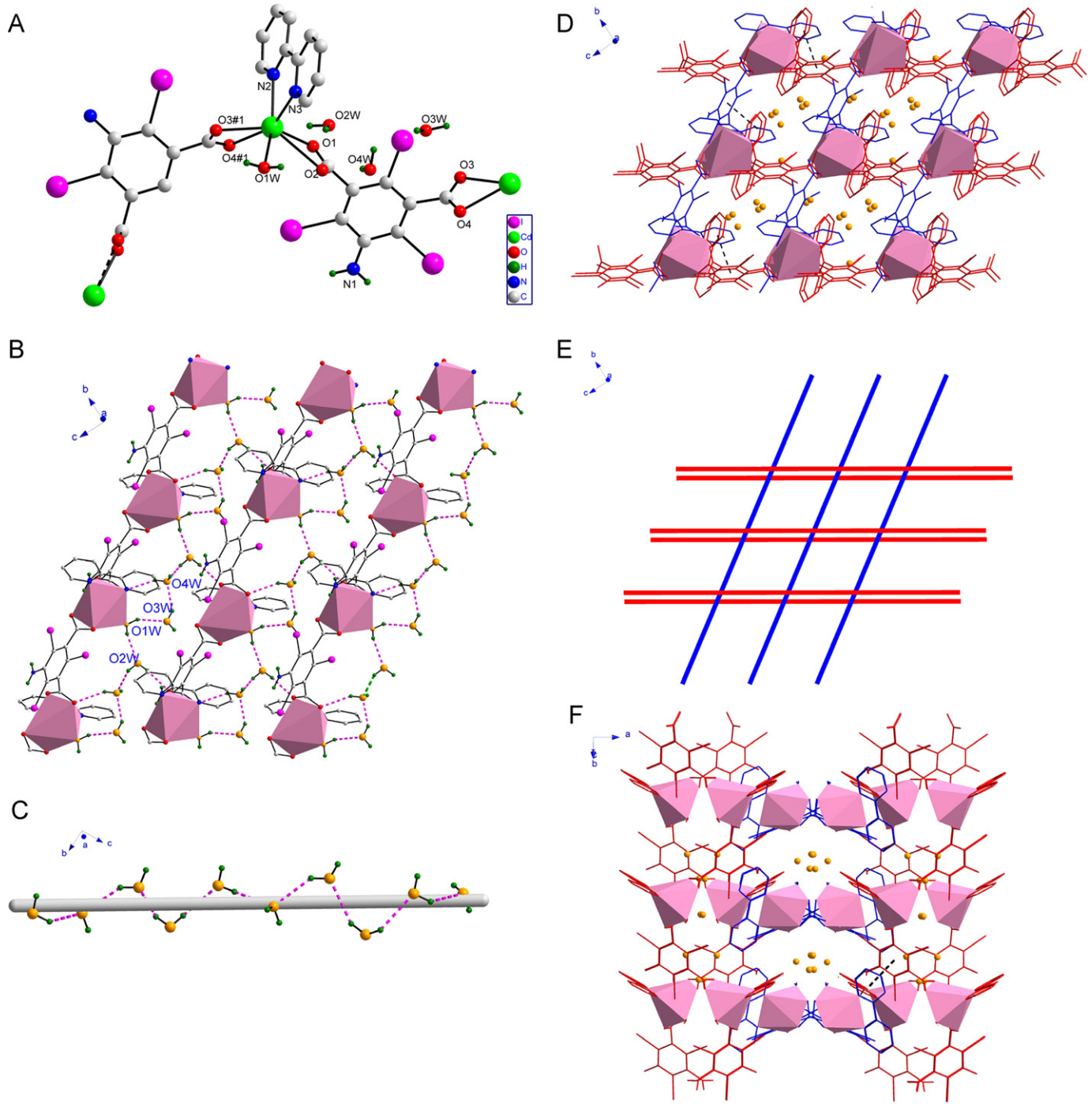

Fig. 2. (A) View of the coordination geometry of the Cd(II) ion in **2**. Symmetry transformations: #1 $-x+3/2, y+1/2, z+1/2$. (B) 1D H-bonded helical water chain with 2_1 helice represented by the gray solid line. (C) 2D supramolecular layer. (D) 3D supramolecular MOF with 1D channels running along [1 0 0]. (E) Schematic representation of 3D supramolecular MOF along [1 0 0], where the solid lines represent the 2_1 helices of the helical chains. (F) 3D supramolecular MOF with 1D channels running along [0.03 −5.32 12.04].

bridges two Mn(II) centers in the bismonodentate (k^1)–(k^1)–μ_2 bridging fashion to form a helical chain with 2_1 helice (Scheme 1) with the intrachain Mn…Mn distance of 9.294(3) Å, whereas the closest interchain Mn…Mn distance is 9.762(9) Å. This is common. However, at a closer look there are some noteworthy features in this structure. The chains run along the *b*-axis. There are right(P)- and left(M)-handed helices in **4** (Fig. 4B). Since the right(P)- and left(M)-handed helices are alternatively arranged, the whole network is therefore racemic. The centroid–centroid distance of the parallel aromatic rings of $ATIBDC^{2-}$ and phen within the chain is 3.676(2) Å, which indicates the existence of strong intrachain $\pi\ldots\pi$ stacking interaction. Interestingly, helical chains further recognize each other through the strong C27–H27…π [3.112(2) Å] and the offset $\pi\ldots\pi$ stacking interactions between the phen ligands of the nearest chains (the centroid–centroid distance: 3.740(3) Å). If these strong $\pi\ldots\pi$ stacking contacts [17] are also considered, then the [Mn(phen)] sections behave as the three-connected nodes. Thus, a 2D network with (6,3) topology is given (Fig. 4C).

Further investigation on the crystal packing indicates that 2D layers are arranged in a parallel fashion along [1 0 0] direction

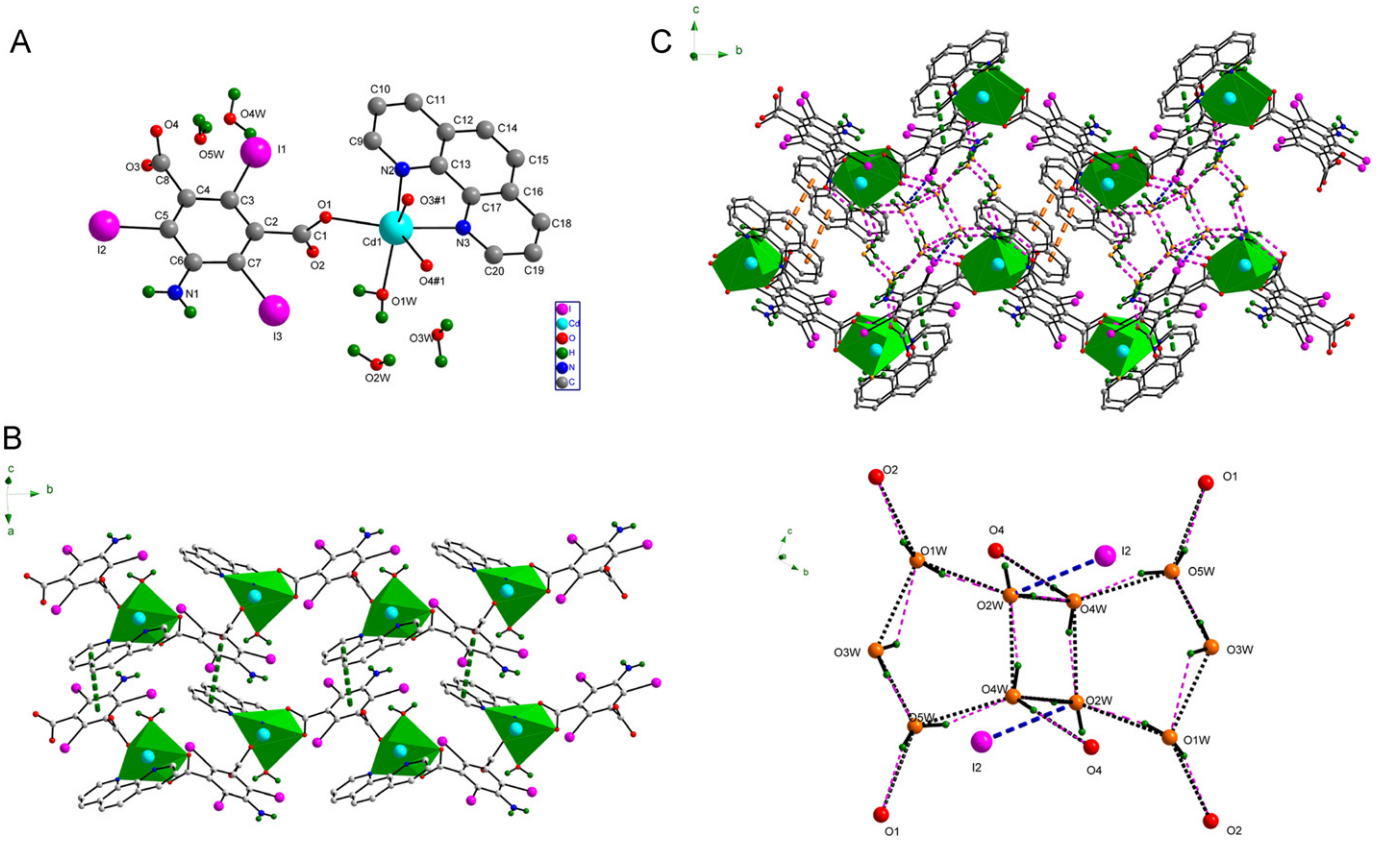

Fig. 3. (A) The coordination environment of Cd(II) in **3**. Symmetry operator: #1 $-x+1$, $y+1/2$, $-z+1/2$. (B) 2D supramolecular array *via* $\pi\ldots\pi$ stacking interactions between the 1D helical chains. (C) (Top): A view of the open 3D supramolecular framework showing hydrogen-bonded water clusters, hydrogen and halogen bonding as well as the offset $\pi\ldots\pi$ stacking interactions connecting the 2D supramolecular layers. (Bottom): Perspective view of the $(H_2O)_{10}$ with a new configuration and its coordination environment, showing the H-bonding and halogen bonding modes.

and assembled into 3D MOF with 1D channels directed by the interlayer C7–I3$\ldots\pi$ [3.805(4) Å] interaction, in which the guest H_2O molecules are accommodated (Fig. 4D). It is really rare that the C–I$\ldots\pi$ interaction acts as the directing force of 3D supramolecular packing.

The hydrogen bonding pattern shows fascinating characteristics in the structure. Five lattice water molecules (O1W, O2W, O3W, O4W, O5W) and their centrosymmetric equivalents (O1Wa, O2Wa, O3Wa, O4Wa, O5Wa) together assemble into a chair-like hydrogen-bonded decameric water cluster (Fig. 4F). The $(H_2O)_{10}$ cluster is of particular interest because this is the smallest unit of naturally occurring cubic ice and so called "molecular ice" [19]. Each chairlike decameric water cluster is formed by a quasiplanar cyclic hexamer (O1WO3WO4WO1WaO3WaO4Wa) and four pendent water molecules (O2W, O5W, O2Wa, O5Wa). It should be interesting to note that O2W and O5W lie in the back region of the "chair", the quasiplanar six-membered ring locates in the "seat", O2Wa and O5Wa being the "legs". The bridging parts between the "seats" and the "back" and the "legs" of the "chair" are O5W–H51…O4W, O3W–H32…O2W and O5Wa–H51a…O4Wa, O3Wa–H32a…O2Wa, respectively (Table S2).

In the $(H_2O)_{10}$ cluster, the average O…O separation within the hexameric core is 2.942 Å, which is comparable to the average O…O contact of *ca.* 2.85 Å found in liquid water but longer than the corresponding value of 2.759 Å in hexagonal ice (I_h) [16]. The average O…O…O angle in the quasiplanar six-membered R6 ring (O1WO3WO4WO1WaO3WaO4Wa) is 118.8°, which is larger than the value of 109.3° in the hexagonal ice [20]. The two uncoordinated symmetrical O2 atoms from two carboxylate groups further double bridge the adjacent $(H_2O)_{10}$ subunits through the hydrogen bonds O1W–H11…O2 and O3W–H31…O2. Thus, a novel 1D hydrogen-bonded helical tape featuring the alternative $(H_2O)_{10}$ units were formed. Hydrogen bonding between the water molecules and uncoordinated oxygen atom O4 in the carboxylate O3C2O4 group (O5W–H52…O4 and O2W–H21…O4) serves to further anchor the water cluster to the coordination polymer matrix (Fig. 4E).

All the five lattice water molecules behave as an acceptor as well as a donor in the hydrogen bonding scheme. In addition, both O1W and O4W are further halogen-bonded to I1 and I2 atoms [I2…O1W 3.313(3) Å, I1…O4W 3.299(5) Å], respectively. These halogen bonds provide additional stabilization of the crystal structure. Thus, O1W, O3W, and O4W show tetracoordination, O2W exhibits tricoordination, and O5W possesses two-coordination.

So, each decameric water cluster is bound to the host lattice through both hydrogen bonds and halogen bonds. Therefore, it appears that the decameric water cluster acts as a template around the pack of the chains.

To the best of our knowledge, such a chair-like conformation of decameric water cluster is also reported for the first time [19].

3.3. Discussion of the structures

From the above-mentioned structural descriptions, it can be seen that the auxiliary chelating ligands have great influence on the chain structures as well as the crystal packing diagrams of the Cd(II) complexes. Supramolecular interactions (hydrogen bonding, halogen bonding, and $\pi\ldots\pi$ interactions) play important roles in the assembly of supramolecular networks **1**–**4**. It should be emphasized that the halogen bonding (C–I$\ldots\pi$ in **1**, C–I…O/N in **1**,

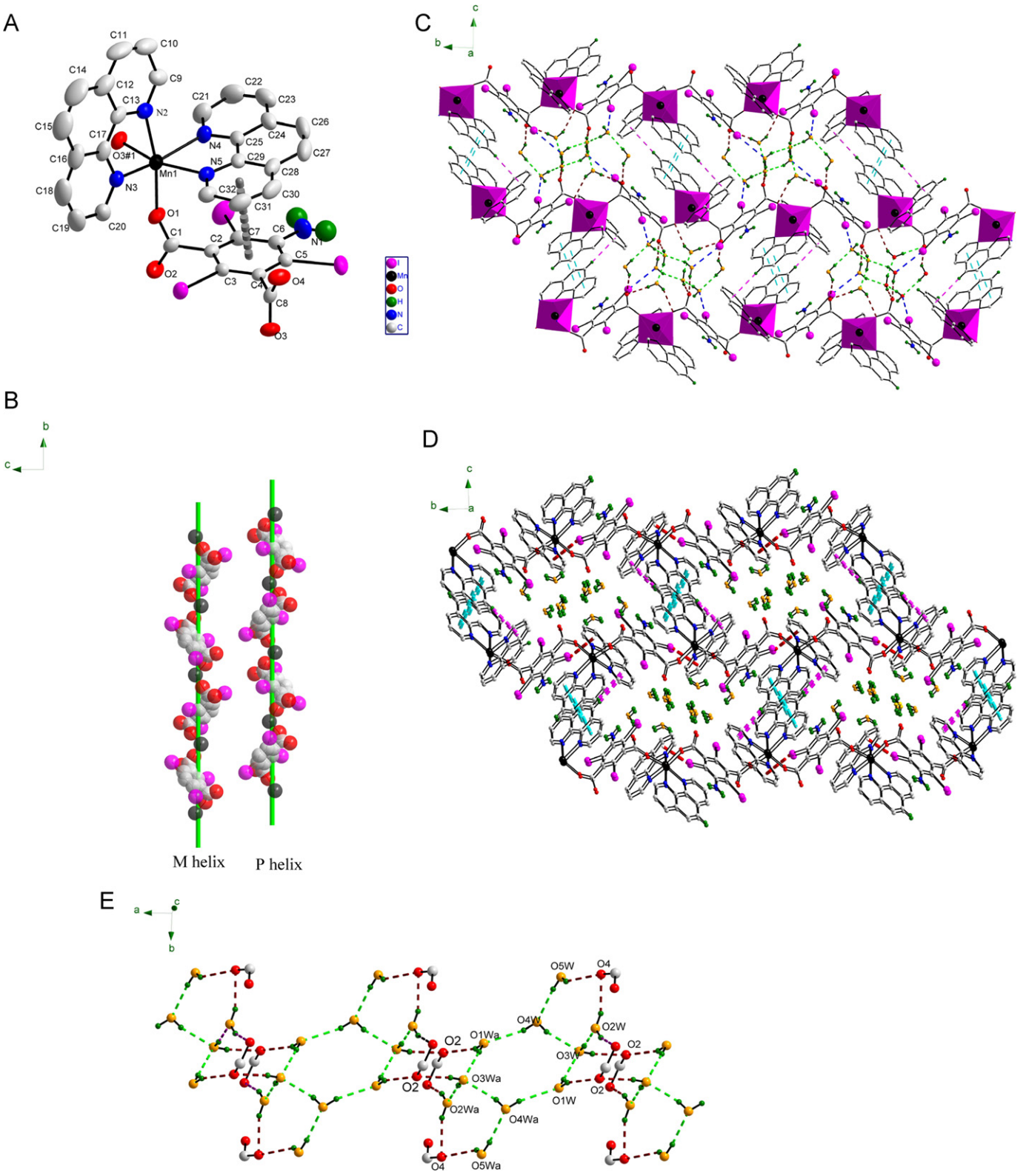

Fig. 4. (A) The coordination environment of Mn(II) in **4**, the dashed gray line represents intrachain $\pi\ldots\pi$ stacking interaction. Symmetry operator: #1 $-x+1$, $y+1/2$, $-z+1/2$. (B) Left-handed helix (M helix) and right-handed helix (P helix), where the solid green line represents 2_1 helice. (C) 2D supramolecular layer, showing the role of water molecules in connecting helical chains with the C–I…O (blue) and O–H…O (green) contacts. The $\pi\ldots\pi$ and C–H…π interactions were represented by the turquiose and pink dashed lines, respectively. (D) 3D MOF directed by the C–I…π halogen bond (red) between the 2D supramolecular layers. (E) 1D hydrogen-bonded helical tape featuring the alternative decameric units $(H_2O)_{10}$ with a new configuration. (For interpretation of the references to color in this figure legend, the reader is referred to the web version of this article.)

3, and **4**) acts as one of the driving forces of 3D supramolecular packing. The successful examples presented here reveal that the I atoms in H_2ATIBDC play important roles in the supramolecular assembly. So, it is a feasible method to construct supramolecular networks by introducing the I atom into aromatic polycarboxylate ligands.

Metal centers also have great effect on the crystalline architectures of this series of compounds. When the auxiliary ligand is phen, Cd(II) favors to form the metal to phen ratio of 1:1 complex **3** while Mn(II) forms the metal to phen ratio of 1:2 complex **4**. The packing diagram of **1** is quite different from that of **2** although these two complexes exhibit the same ratio of M:ATIBDC^{2-}:2, 2′-bipy in their formula and show similar chain structures. This may be due to the different coordination behavior of the metal nodes.

3.4. IR spectra and thermal stability

The FT-IR spectral data show features attributable to the carboxylate stretching vibrations of **1**–**4**. The absence of bands in the range of 1680–1760 cm^{-1} indicates the complete deprotonation of H_2ATIBDC in all the materials. The characteristic bands of the carboxylate groups appear in the range 1552–1598 cm^{-1} for the asymmetric stretching and 1384–1490 cm^{-1} for the symmetric stretching. The broad band at *ca.* 3300 cm^{-1} corresponds to the vibration of the –NH_2 group in the ATIBDC^{2-} ligand, methanol, and water molecules in the corresponding complexes **1**–**4** [21].

To study the thermal stability of the materials, the thermogravimetric analysis (TG) was performed on all samples under a nitrogen atmosphere in flowing N_2 with a heating rate of 10 °C min^{-1} (Fig. 5). TGA of **1** suggests that the release of the guest molecules begins at about 20 °C. The total weight loss (9.22%) up to 200 °C corresponds to the loss of all the lattice water and methanol molecules (calcd. 10.03%). In **2**, the 7.68% weight decrease from 40 to 120 °C corresponds to the loss of one coordinated water and three lattice water molecules (calcd. 8.09%). The second decomposition process begins from 280 °C. For **3**, the first-step weight loss of 8.95% (calcd. 9.62%) from 50 to 180 °C corresponds to the removal of five water molecules. Complex **4** exhibits a weight loss of 8.57% at 50–180 °C, corresponding to the loss of all the water molecules (calcd. 8.02%). The weight loss beginning at 180 °C corresponds to the decomposition of the framework.

3.5. Circular dichroism measurement

Solid-state circular dichroism (CD) spectrum was measured on KBr pellet for compound **1** (Fig. S1). Clearly, compound **1** exhibits positive Cotton effect, which further reveals that it exhibits the homochirality.

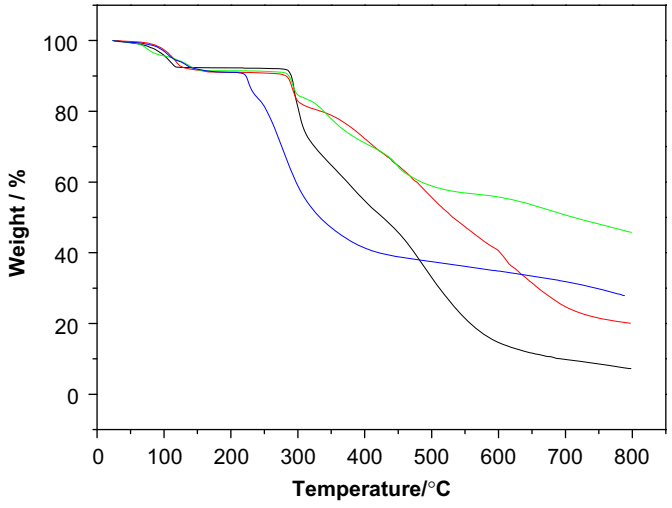

Fig. 5. TG curves of **1** (blue), **2** (black), **3** (red), and **4** (green). (For interpretation of the references to color in this figure legend, the reader is referred to the web version of this article.)

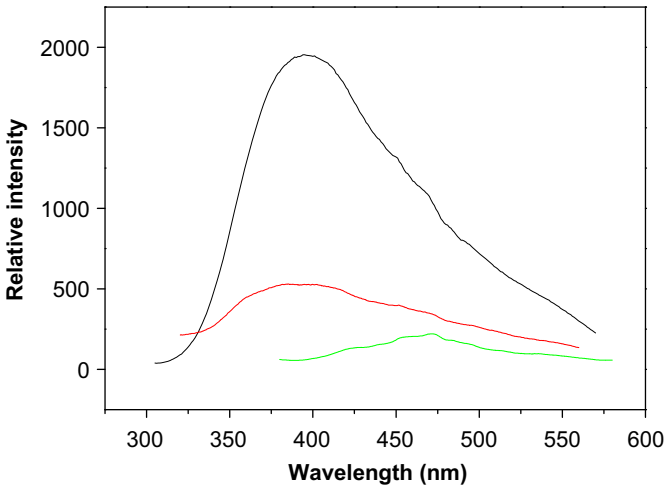

Fig. 6. Solid-state fluorescence emissions recorded at room temperature for H_2ATIBDC (green), **2** (black), and **3** (red). The excitation wavelength (λ_{ex}) is 290 nm for H_2ATIBDC, **2**, and **3**. (For interpretation of the references to color in this figure legend, the reader is referred to the web version of this article.)

3.6. Fluorescence properties of the Cd(II) complexes in the solid state

Polymeric d^{10} metal complexes with aromatic ligands may be considered as good candidates for potential photoactive materials because of their structural stability and insoluble nature. Thus, solid state fluorescent properties of the Cd(II) complexes **2** and **3** have been investigated at room temperature. To well-compare the photoluminescence intensity of these two compounds with the free H_2ATIBDC acid, we determined all the emission spectra with the same excitation wavelength (λ_{ex}=290 nm) (Fig. 6). The free acid H_2ATIBDC exhibits the emission with the peak maxima occurring at 473 nm and a shoulder at about 453 nm (λ_{ex}=290 nm). The complexes **2** and **3** show significant blue-shifted luminescence with emission maxima at 380 nm in the solid state, which may be ascribed to the ligand-to-metal charge transfer (LMCT). The stronger fluorescent intensity of **2** than that of **3** may be attributed that **2** has fewer water molecules than **3**.

Complexes **2** and **3** may be good candidates for solvent-resistant photoactive fluorescent materials because they are almost insoluble in common polar and nonpolar solvents.

4. Conclusion

In conclusion, one homochiral and three achiral 1D coordination polymers **1**–**4** with the ATIBDC^{2-} ligand have been prepared and characterized. They possess extended 3D supramolecular architectures with the aid of various supramolecular driving forces. Remarkably, two new configurations of water decamer have been observed in **3** and **4**. The features of the ATIBDC^{2-} ligand, strong ability of hydrogen/halogen bonding as well as various connection modes, have been embodied in these complexes. The studies further reveal that the halogen bonds (C–I…π and C–I…O/N) are useful tools to construct supramolecular networks. The use of halogen bonding as supramolecular driving force opens up new insights to materials design and supramolecular synthesis. Initially, it is likely that the interest can be stimulated to develop a novel family of iodine-substituted aromatic polycarboxylate ligands as supporting spacers. The fluorescence properties of the polymeric Cd(II) complexes can be tuned

by the auxiliary chelating ligands. Complexes **2** and **3** may be used as photoactive materials. Further synthesis of the related supramolecular complexes with the series of I-substituted aromatic polycarboxylate ligands is underway.

Supplementary material

Crystallographic data have been deposited with the Cambridge Crystallographic Data Center with CCDC reference numbers: 730068 (**1**), 730392 (**2**), 729548 (**3**), and 729621 (**4**). Copies of this information may be obtained free of charge from the director, CCDC, 12 Union Road, Cambridge CB2 IEZ, UK (e-mail: deposit@ccdc.cam.ac.uk or www:http://www.ccdc.cam.ac.uk).

Acknowledgment

The authors gratefully acknowledge the Key Laboratory of Environmental Material and Environmental Engineering of Jiangsu Province and Postdoctoral Foundation of Yangzhou University for the financial support of this work.

Appendix A. Supplementary materials

Supplementary materials associated with this article can be found in the online version at doi:10.1016/j.jssc.2011.03.0502.

References

[1] (a) F.N. Keutsch, J.D. Cruzan, R.J. Saykally, Chem. Rev. 103 (2003) 2533;
(b) A. Müller, E. Krickemeyer, H. Bögge, M. Schmidtmann, B. Botar, M.O. Talismanova, Angew. Chem. Int. Ed. 42 (2003) 2085;
(c) J.M. Ugalde, I. Alkorta, J. Elguero, Angew. Chem. Int. Ed. 39 (2000) 717;
(d) C.J. Gruenloh, J.R. Carney, C.A. Arrington, T.S. Zwier, S.Y. Fredeicks, K.D. Jordan, Science 276 (1997) 1678.
[2] (a) M. Mascal, L. Infantes, J. Chisholm, Angew. Chem. Int. Ed. 45 (2006) 32;
(b) J.K. Gregory, D.C. Clary, K. Liu, M.G. Brown, R.J. Saykally, Science 275 (1997) 814;
(c) K. Liu, M.G. Brown, C. Carter, R.J. Saykally, J.K. Gregory, D.C. Clary, Nature 381 (1996) 501;
(d) J.D. Cruzan, L.B. Braly, K. Liu, M.G. Brown, J.G. Loeser, R.J. Saykally, Science 271 (1996) 59;
(e) K. Nauta, R.E. Miller, Science 287 (2000) 293;
(f) L. Infantes, S. Motherwell, CrystEngComm. 4 (2002) 454.
[3] (a) A. Morsali, M.Y. Masoumi, Coord. Chem. Rev. 253 (2009) 1882;
(b) J. An, S.J. Geib, N.L. Rosi, J. Am. Chem. Soc. 132 (2010) 38;
(c) R. Kitaura, K. Fujimoto, S. Noro, M. Kondo, S. Kitagawa, Angew. Chem. Int. Ed. 41 (2002) 133;
(d) L. Brammer, Chem. Soc. Rev. 33 (2004) 476;
(e) B.H. Ye, M.L. Tong, X.M. Chen, Coord. Chem. Rev. 249 (2005) 545;
(f) L. Carlucci, G. Ciani, D.M. Proserpio, Coord. Chem. Rev. 246 (2003) 247.
[4] (a) F.A.A. Paz, J. Klinowski, Chem. Commun. (2003) 1484;
(b) Y. Zhang, J. Li, J. Chen, Q. Su, W. Deng, M. Nishiura, T. Imamoto, X. Wu, Q. Wang, Inorg. Chem. 39 (2000) 2330;
(c) G.R. Desiraju, Crystal Design: Structure and Function, Perspectives in Supramolecular Chemistry, Wiley, Chichester, 2003 (vol. 6);
(d) A.G. Wong-Foy, A.J. Matzger, O.M. Yaghi, J. Am. Chem. Soc. 128 (2006) 3494;
(e) J. Lee, O.K. Farha, J. Roberts, K.A. Scheidt, S.T. Nguyen, J.T. Hupp, Chem. Soc. Rev. 38 (2009) 1450;
(f) M.H. Alkordi, Y. Liu, R.W. Larsen, J.F. Eubank, M. Eddaoudi, J. Am. Chem. Soc. 130 (2008) 12639;
(g) G. Férey, Chem. Soc. Rev. 37 (2008) 191.
[5] (a) Y.Y. Niu, H.G. Zheng, H.W. Hou, X.Q. Xin, Coord. Chem. Rev. 248 (2004) 169;
(b) J. Heo, Y.M. Jeon, C.A. Mirkin, J. Am. Chem. Soc. 129 (2007) 7712;
(c) J. Luo, H. Xu, Y. Liu, Y. Zhao, L.L. Daemen, C. Brown, T.V. Timofeeva, S. Ma, H.-C. Zhou, J. Am. Chem. Soc. 130 (2008) 9626;
(d) O.R. Evans, W. Lin, Acc. Chem. Res. 35 (2002) 511;
(e) X.H. Bu, W. Chen, S.L. Lu, R.H. Zhang, D.Z. Liao, W.M. Shionoya, M. Bu, F. Brisse, J. Ribas, Angew. Chem. Int. Ed. 40 (2001) 3201;
(f) L.J. Murray, M. Dincă, J.R. Long, Chem. Soc. Rev. 38 (2009) 1294;
(g) X.-H. Zhou, Y.-H. Peng, X.-D. Du, C.-F. Wang, J.-L. Zuo, X.-Z. You, Cryst. Growth Des. 9 (2009) 1028;
(h) Y.-L. Zhou, M.-C. Wu, M.-H. Zeng, H. Liang, Inorg. Chem. 48 (2009) 10146.
[6] (a) C.-L. Chen, B.-S. Kang, C.-Y. Su, Aust. J. Chem. 59 (2006) 3;
(b) B.D. Wagner, G.J. McManus, B. Moulton, M.J. Zaworotko, Chem. Commun. (2002) 2176;
(c) J. Yang, J.-F. Ma, Y.-Y. Liu, J.-C. Ma, S.R. Batten, Inorg. Chem. 46 (2007) 6542;
(d) C.B. Aakeröy, N.R. Champness, C. Janiak, CrystEngComm. 12 (2010) 22.
[7] (a) A.M. Beatty, Coord. Chem. Rev. 246 (2003) 131;
(b) X.-P. Li, J.-Y. Zhang, M. Pan, S.-R. Zheng, Y. Liu, C.-Y. Su, Inorg. Chem. 46 (2007) 4617;
(c) O.M. Yaghi, H. Li, T.L. Groy, Inorg. Chem. 36 (1997) 4292;
(d) D.F. Sava, V.Ch. Kravtsov, J. Eckert, J.F. Eubank, F. Nouar, M. Eddaoudi, J. Am. Chem. Soc. 131 (2009) 10394.
[8] F. Dai, H. He, D. Gao, Fei Ye, X. Qiu, D. Sun, CrystEngComm. 11 (2009) 2516.
[9] K. Rissanen, CrystEngComm. 10 (2008) 1107.
[10] (a) K.M. Guckian, B.A. Schweitzer, R.X.-F. Ren, C.J. Sheils, D.C. Tahmassebi, E.T. Kool, J. Am. Chem. Soc. 122 (2000) 2213;
(b) Y. Kim, J.H. Geiger, S. Hahn, P.B. Sigler, Nature 365 (1993) 512.
[11] (a) F. Dai, H. He, D. Sun, J. Am. Chem. Soc. 130 (2008) 14064;
(b) F. Dai, H. He, D. Sun, Inorg. Chem. 48 (2009) 4613;
(c) F. Dai, H. He, X. Zhao, Y. Ke, G. Zhang, D. Sun, CrystEngComm. 12 (2010) 337.
[12] K.-L. Zhang, Y. Chang, C.-T. Hou, G.-W. Diao, R. Wu, S.W. Ng, CrystEngComm. 12 (2010) 1194.
[13] G.M. Sheldrick, SHELXL 97. Programs for Crystal Structure Analysis (Release 97-2), 1997, University of Götinggen, Germany.
[14] (a) O. Sereda, H. Stoeckli-Evans, O. Dolomanov, Y. Filinchuk, P. Pattison Cryst., Growth Des. 9 (2009) 3168;
(b) E.C. Constable, Nature 346 (1990) 314;
(c) R. Robson, J. Chem. Soc. Dalton Trans. (2000) 3735;
(d) G.R. Desiraju, J. Chem. Soc. Dalton Trans. (2000) 3745;
(e) A. von Zelewsky, O. Mamula, J. Chem. Soc. Dalton Trans. (2000) 219;
(f) Y.-R. Xie, R.-G. Xiong, X. Xue, X.-T. Chen, Z. Xue, X.-Z. You, Inorg. Chem. 41 (2002) 3323.
[15] M. Felloni, A.J. Blake, P. Hubberstey, C. Wilson, M. Schröder, Cryst. Growth Des. 9 (2009) 4685.
[16] D. Eisenberg, W. Kauzmann, The Structure and Properties of Water, Oxford University Press, Oxford, 1969.
[17] C.-Y. Niu, B.-L. Wu, X.-F. Zheng, H.-Y. Zhang, H.-W. Hou, Y.-Y. Niu, Z.-J. Li, Cryst. Growth Des. 8 (2008) 1566.
[18] J.D. Cruzan, M.R. Viant, M.G. Brown, R.J. Saykally, J. Phys. Chem. A 101 (1997) 9022.
[19] (a) L.J. Barbour, G.W. Orr, J.L. Atwood, Nature 393 (1998) 671;
(b) L.J. Barbour, G.W. Orr, J.L. Atwood, Chem. Commun. (2000) 859;
(c) M. Yoshizawa, T. Kusukawa, M. Kawano, T. Ohhara, I. Tanaka, K. Kurihara, N. Niimura, M. Fujita, J. Am. Chem. Soc. 127 (2005) 2798;
(d) A. Michaelides, S. Skoulika, E.G. Bakalbassis, J. Mrozinski, Cryst. Growth. Des. 3 (2003) 487;
(e) B.C.R. Sansam, K.M. Anderson, J.W. Steed, Cryst. Growth. Des. 7 (2007) 2649;
(f) Y. Jin, Y.X. Che, J.M. Zheng, Inorg. Chem. Commun. 10 (2007) 514;
(g) Y.Y. Karabach, A.M. Kirillov, M.F.C. De Silva, M.N. Kopylovich, A.J.L. Pombeiro, Cryst Growth Des. 6 (2006) 2200;
(h) S.K. Ghosh, P.K. Bharadwaj, Eur. J. Inorg. Chem. (2006) 1341;
(i) Y. Li, L. Jiang, X.L. Feng, T.B. Lu, Cryst. Growth Des. 6 (2006) 1074;
(j) O. Ermer, J. Neudörfl, Chem. Eur. J. 7 (2001) 4961;
(k) L.-Y. Wang, Y. Yang, K. Liu, B.-L. Li, Y. Zhang, Cryst. Growth Des. 8 (2008) 3902;
(l) M. Estrader, J. Ribas, V. Tangoulis, X. Solans, M. Font-Bardia, M. Maestro, C. Diaz, Inorg. Chem. 45 (2006) 8239.
[20] C. Janiak, J. Chem. Soc., Dalton Trans. (2000) 3885.
[21] K. Nakamoto, Infrared and Raman Spectra of Inorganic and Coordination Compounds, 4th edn., Wiley, New York, 1986 (p. 231).